# Evolution of the spatiotemporal pattern of PM2.5 concentrations in China – a case study from the Beijing-Tianjin-Hebei region

Dan Yan[1,2,3], Yalin Lei[1,2*], Yukun Shi[4], Qing Zhu[5], Li Li[1,2], Zhien Zhang[6]

1. School of Humanities and Economic Management, China University of Geosciences, Beijing, 100083, China

2. Key Laboratory of Carrying Capacity Assessment for Resource and Environment, Ministry of Land and Resources, Beijing, 100083, China

3. Research Center for Transition and Development of Resource-exhausted cities, Hubei Normal University,Huangshi, 435002, China.

4. Adam Smith Business School, University of Glasgow, Glasgow G12 8QQ, UK

5. Chinese Academy of Land & Resource Economics, Beijing, 101149, China

6. School of Chemistry and Chemical Engineering, Chongqing University of Technology, 400054, China

**Abstract:**

Atmospheric haze pollution has become a global concern because of its severe effects on human health and the environment. The Beijing-Tianjin-Hebei urban agglomeration is located in northern China, and its haze is the most serious in China. The high concentration of PM2.5 is the main cause of haze pollution, and thus investigating the temporal and spatial characteristics of PM2.5 is important for understanding the mechanisms underlying PM2.5 pollution and for preventing haze. In this study, the PM2.5 concentration status in 13 cities from the Beijing-Tianjin-Hebei region was statistically analyzed from January 2016 to November 2016, and the spatial variation of PM2.5 was explored via spatial autocorrelation analysis. The research yielded three overall results. (1) The distribution of PM2.5 concentrations in this area varied greatly during the study period. The concentrations increased from late autumn to early winter, and the spatial range expanded from southeast to northwest. In contrast, the PM2.5 concentration decreased rapidly from late winter to early spring, and the spatial range narrowed from northwest to southeast. (2) The spatial dependence degree, by season from high to low, was in the order winter, autumn, spring, summer. Winter (from December to February of the subsequent year) and summer (from June to August) were, respectively, the highest and lowest seasons with regard to the spatial homogeneity of PM2.5 concentrations. (3) The PM2.5 concentration in the Beijing-Tianjin-Hebei region has significant spatial spillovers. Overall, cities far from Bohai Bay, such as Shijiazhuang and Hengshui, demonstrated a high-high concentration of PM2.5 pollution, while coastal cities, such as Chengde and Qinhuangdao, showed a low-low concentration.

**Keywords:** Beijing-Tianjin-Hebei region; Air pollution; PM2.5 concentration; spatial autocorrelation analysis.

## 1. Introduction

China's serious haze problem has aroused widespread concern among the public. The increase in the concentrations of particulates (including PM10 and PM2.5) in the atmosphere is the main cause of haze production (Xu and Lin, 2016; Hsu et al., 2017; Liao et al., 2017; Liu et al., 2015a). Studies have shown that high levels of PM2.5 and PM10 are closely linked to high concentrations of fungi and bacteria in the air, which can cause serious harm to humans (Liu et al., 2017a; Liu et al., 2017b; Liu et al., 2015b). In 2012, China issued newly revised ambient air quality standards; PM2.5, regarded as a routine indicator of atmospheric pollution, was included in the new standard and has become the key focus of atmospheric pollution research. PM2.5 refers to fine particles with a dynamic diameter of less than 2.5 μm. These particles are composed of a wide variety of complex chemical substances emitted from various natural and anthropogenic sources (Alves et al., 2012; Wang et al., 2012; Zhao et al., 2014). A high concentration of PM2.5 not only significantly reduces atmospheric visibility but also leads to increased incidences of respiratory and cardiovascular diseases (Dockery et al., 1993; Li et al., 2016; Chalbot et al., 2014; Hu et al., 2014). At the beginning of 2013, China suffered from the most serious fog and haze pollution since the start of observational records, and this rare continuous high-intensity air pollution swept the middle and eastern parts of China. The most serious pollution occurred in the Beijing-Tianjin-Hebei (BTH) region, where the daily PM2.5 concentration reached 500 μg/m$^3$(Wang et al., 2014). The BTH region is China's political and cultural center and is an important core area of North China's economy. Since the 1980s, the economy, society and culture of the BTH region have developed remarkably. The gross domestic product (GDP) increased approximately seven-fold from 593.342 billion yuan in 1980 to 4715.233 billion yuan in 2013(Beijing

Statistical Yearbook 2014; Tianjin Statistical Yearbook 2014; Hebei Economic Yearbook 2014). However, at the same time, serious air pollution exists in the 13 cities within the BTH region. According to the Ministry of Environmental Protection, the worst ten cities in terms of air quality in 2015 were Baoding, Xingtai, Hengshui, Tangshan, Zhengzhou, Jinan, Handan, Shijiazhuang, Langfang and Shenyang. Seven of these cities are within the BTH region. The haze pollution in the BTH region cannot be overlooked, and haze governance has become the top priority for the BTH region (Cai et al., 2017). Therefore, studying the temporal and spatial characteristics of PM2.5 in this region has great practical value. Understanding the spatial variation of the PM2.5 concentration will not only add to our knowledge of the mechanism of air pollution but also provide a scientific reference for implementing targeted control measures.

The consumption of fossil energy, such as coal and oil, generates a large amount of waste gas, which affects the climate and endangers human health. Therefore, energy-saving emission reduction is crucial (Ma et al., 2017a; Yan et al., 2017). Many scholars have focused on carbon emissions reduction in their research (Shuai et al., 2017; Ma et al., 2017b; Ma et al., 2017c), and now society as a whole is beginning to pay attention to the haze issue in China.

Existing research on the haze problem mainly focuses on two aspects. Initially, most scholars analyzed the composition of PM2.5 from the physical and chemical perspectives (Bates and Sizto, 1987; Hussain et al., 2013; Jansen et al., 2014) and concluded that PM2.5 was mainly composed of industrial waste gas, automobile and machine exhaust, cooking oil smoke and dust. These pollutants are closely related to socioeconomic factors such as GDP, population, energy consumption and industrial infrastructure. In light of these findings, a large number of studies have focused on the economic and social drivers of the PM2.5 concentration. For example, based on the data on the PM2.5 concentration and the air quality index (AQI) in 73 Chinese cities in 2013, Hao and Liu (2016) analyzed the influencing factors of the PM2.5 concentration in China's cities and discussed how economic and social development could affect air quality. Their results show that the relationship between the PM2.5 concentration and GDP per capita exhibits an inverted U shape and that car ownership and secondary industry have significant effects on the PM2.5 concentration. Luo et al. (2017) explored the driving factors of the PM2.5 concentration in China using a geographical regression weighting model, which confirmed the existence of the inverted U-shaped environmental Kuznets curve (EKC) for air quality and that the potential influencing factors of each significant area were different. By using the input-output framework and structural decomposition analysis, Guan et al. (2014) studied the socioeconomic drivers of China's primary PM2.5 emissions and found that export is the only final demand category that led to emission growth between 1997 and 2010. The embodied PM2.5 emissions from Chinese exports are mainly driven by consumption in OECD countries. The second studied aspect is the spillover effects of interregional air pollution. $SO_2$, $NO_X$ and soot are often used as proxy variables for air pollution (Civan et al., 2015; Moroń et al., 2015; Zhao et al., 2017).Spatial variability analysis in geography is an important basis for simulating the spatial distribution of variables and revealing the spatial effects of variables (Liu et al., 2016; Zuo et al., 2015). Furthermore, spatial autocorrelation analysis is an important technical method that has recently been applied to the field of environmental pollution, particularly air pollution. For example, Zhang et al. (2016) examined the spatial clustering types of $CO_2$ emission efficiency in 30 provinces in China and confirmed that there is indeed a spatial spillover effect among Chinese provinces. To gain insight into the characteristics of air pollution, Wu et al. (2017) explored the characteristics and determinants of PM2.5 pollution in China using spatial econometrics. Yan et al. (2017) used Moran's index to examine the spatial effects of the power industry in various regions of China. The empirical results showed that there is indeed a significant spatial agglomeration effect between carbon emission efficiencies, mainly for high-high and low-low agglomeration types.

The concentration of air pollutants is affected by the intensity of emission sources and by terrain and meteorological conditions; furthermore, it has remarkable temporal and spatial variability. In China, PM2.5 started to attract attention in 2012. The majority of the literature is devoted to the analysis of the formation of fog and haze and to the chemical composition of PM2.5 or its influencing factors at the national scale, whereas studies on the distribution pattern of PM2.5 concentrations on the urban scale are relatively rare. Compared with previous research, this study has two main contributions. Thematically, through the PM2.5 pollution index, we analyze the spillover effect of haze between different cities in the BTH urban agglomeration. The results will allow the general public to clearly understand the spatiotemporal rules of haze pollution in this urban agglomeration and provide new evidence for haze management. Methodologically speaking, abandoning the geospatial homogeneity hypothesis in spatial econometrics would better fit the real situation of the PM2.5 concentration and facilitate the examination of the propagation path of haze pollution. Specifically, we collected data on daily PM2.5 concentrations in 2016 in 13 cities located within the BTH region and studied the spatial autocorrelations and aggregation patterns of PM2.5 concentrations during different seasons. The results were intended to provide a basis for simulating PM2.5 concentrations in the region, elucidating the underlying factors contributing to this pollution, and devising an effective monitoring point layout.

The remaining parts of this paper are organized as follows. The second section describes the data source and model description. In the third section, we present the temporal and spatial variation of PM2.5 concentrations in the BTH region. The fourth section describes and discusses the results of spatial autocorrelation, which is followed by the final conclusions and policy implications in the fifth section.

## 2. Data and methodology

### 2.1 Overview of the BTH region and data sources

In 2013, China established a total of 612 PM2.5 concentration monitoring sites in 74 cities, and the number of monitoring sites in each city was different. By 2015, the monitoring sites increased to 1436 (Wang et al., 2015). Presently, the sites that monitor the PM2.5 concentration in China are mainly concentrated in the Pearl River Delta, Yangtze River Delta and BTH region. Among these areas, the urban agglomeration of the BTH region suffers from relatively more severe haze pollution than other cities, and some studies have suggested that this was because several coal-based industries, such as coal-fired power plants and steel manufacturing, are stationed in the region (Zhao et al., 2012). This area is adjacent to Bohai Bay and is composed of 13 cities, namely, Beijing, Tianjin, Shijiazhuang, Xingtai, Handan, Hengshui, Baoding, Cangzhou, Langfang, Tangshan, Zhangjiakou, Chengde and Qinhuangdao. The land area of this region is 218,000 square kilometers, and the resident population is approximately 110 million people. Industrialization has greatly bolstered the BTH region's economic development, and the main industrial types are steelmaking, petroleum processing and coking, nuclear fuel processing, building materials manufacturing and chemical manufacturing. The common feature of these industries is high energy consumption; thus, a large amount of atmospheric emissions is produced. In 2015, the total industrial emissions from this region was 4.138 million tons, including dust, sulfur dioxide and nitrogen dioxide. These chemical substances are precursors of sulfate and nitrate of PM2.5.

In this study, the hourly PM2.5 concentration data of the urban air quality monitoring sites in 13 cities in 2016 were obtained from the China Environmental

Monitoring Station as raw data. According to the arithmetic average method, these data from cities or monitoring sites can be calculated as daily averages, monthly averages, quarterly averages and as an annual average within 2016. In accordance with the requirements of the Ambient Air Quality Standard for the effectiveness of air pollutant concentration data, the PM2.5 data were pretreated. First, we removed missing values. Second, when the monthly mean was calculated, the monitoring site was eliminated if the number of daily PM2.5 concentration measurements was less than 27 days in a month. Finally, a small number of abnormal monitoring points were eliminated (such as hourly PM2.5 concentrations greater than 900 $\mu g.m^{-3}$ or hourly PM2.5 concentrations less than 0).

## 2.2 Spatial interpolation method

The spatial interpolation method is often used to convert point scale data into a continuous surface scale. Additionally, this method helps us better understand the full spatial distribution of variables in the region. The accuracy of the spatial interpolation method is greater than that of remote sensing inversion (Lee S J et al., 2012). Many specific methods are commonly used for spatial interpolation, such as the Inverse Distance Weighted (IDW) method and the Ordinary Kriging method (OK). The accuracy of the estimates using the former method is influenced by the distance to a known point, and the requirements for the dispersion and uniformity of the interpolation points are relatively higher. The latter method will generate the best estimation algorithm for the output surface and will create a comprehensive calculation of the spatial behavior of the interpolation point attribute prior to the generation of the algorithm; thus, the results from the second method are preferable (Zhang et al., 2013). Generally, the OK method can reflect the spatial distribution of PM2.5 more scientifically and the result has second-order stationarity.

## 2.3 Spatial clustering analysis of the PM2.5 concentration based on Moran 's Index

According to the first law of geography, entities with geographical attributes are related with each other. Clustering, random and regular distribution exist, and correlation decreases with distance (Tober, 1970). This phenomenon is called spatial autocorrelation. Spatial autocorrelation statistics can describe the potential interdependence or compactness of variables within the same area. This approach is often used to analyze the spatial agglomeration and trend of geographical elements to provide evidence for exploring spatial and temporal clustering and evolution. The spatial correlation of atmospheric activity may reveal that the values of PM2.5 concentrations in similar areas are statistically close (Wu et al., 2015). Spatial autocorrelation analysis includes global spatial autocorrelation and local spatial autocorrelation, in which the global Moran Index is calculated as follows:

$$I = \frac{n \sum_{i=1}^{n} \sum_{j=1}^{n} w_{ij} Z_i Z_j}{S_o \sum_{i=1}^{n} Z_i^2} \quad (1)$$

where $S_o = \sum_{i=1}^{n} \sum_{j=1}^{n} w_{ij}$, and $w_{ij}$ is the spatial weight matrix; in this paper, the adjacent unit is 1, and the remaining units are zero. The Moran Index is in the range [-1, 1]. A value less than 0, equal to 0, or greater than 0 indicates negative correlation, no correlation or positive correlation, respectively. For the Moran Index, the standardized statistic $Z$ can be used to test the existence of spatial autocorrelation. The formula for the standardized statistic $Z$ is as follows:

$$Z_i = \frac{I - E[I]}{\sqrt{V[I]}} \quad (2)$$

$$\mathrm{E}[I] = -1 \,/\, (n-1) \quad (3)$$

$$\mathrm{V}[I] = E[I^2] - E[I]^2 \quad (4)$$

Among these formulas, at the 0.05 significance level, Z(I)>1.96 indicates positive spatial autocorrelation between PM2.5 spatial units, and -1.96<Z(I)<1.96 indicates that the spatial correlation of PM2.5 concentrations is not obvious. If Z(I)<-1.96, then there is a negative correlation between PM2.5 spatial units, and the attribute value tends to be distributed. Local spatial autocorrelation is used to determine the specific location of spatial agglomeration, and the local Moran Index is calculated as follows:

$$I_i = \frac{X_i - \overline{X}}{S_i^2} \sum_{j=1, j \neq i}^{n} w_{ij} (X_i - \overline{X}) \quad (5)$$

where $X_i$ is the attribute value of $i$, $\overline{X}$ is the average value, and $w_{ij}$ is the spatial weight matrix; then,

$$S_i^2 = \frac{\sum_{j=1, j \neq i}^{n} w_{ij}}{n-1} - \overline{X}^2 \quad (6)$$

The standardized statistic of local Moran Index test is Z[I]:

$$Z_{Ii} = \frac{I_i - E[I_i]}{\sqrt{V[I_i]}} \quad (7)$$

$$\mathrm{E}[I_i] = -1 \,/\, (n-1) \quad (8)$$

$$V[I_i] = E[I_i{}^2] - E[I_i]^2 \quad (9)$$

At the 0.05 significance level, Z>1.96 indicates that cities with high PM2.5 concentrations are surrounded by other cities with high PM2.5 concentrations and that cities with low PM2.5 concentrations are surrounded by other cities with low PM2.5 concentrations. Z<-1.96 indicates that cities with high PM2.5 concentrations are surrounded by cities with low PM2.5 concentrations and that cities with low PM2.5 concentrations are surrounded by cities with high PM2.5 concentrations. When Z=0, the observations demonstrate an independent random distribution.

## 3. The variation and regularity of PM2.5 concentrations in the BTH region

### 3.1 The monthly variation characteristics of PM2.5 concentrations

An investigation of the PM2.5 concentration changes from the cities in the BTH region over the 12 months in 2016 (see Figure 1) reveals that the median monthly PM2.5 concentrations in the 13 cities demonstrate U-shaped oscillations over the entire time period. Specifically, the PM2.5 concentration demonstrated a downward trend from January to May, was overall stable from June to August, and finally increased from October to December. Among the latter months, the highest peak occurred in December and was 147.34 μg.m$^{-3}$; meanwhile, the lowest peak appeared in August and was 38.95 μg.m$^{-3}$. From May to September, the median PM2.5 concentration was under 60 μg.m$^{-3}$; thus, this time represents the highest air quality period in the BTH region within the entire year. In general, PM2.5 concentrations showed significant differences by month. In the winter, PM2.5 pollution is the most severe, but during spring, it begins to decrease and eventually maintains a stable state in the late spring. By the summer, PM2.5 pollution decreases to the lowest level and then again begins to increase during late autumn. It can be reasonably speculated that the PM2.5 concentration value varies with the seasonal weather and forms a cyclical change pattern.

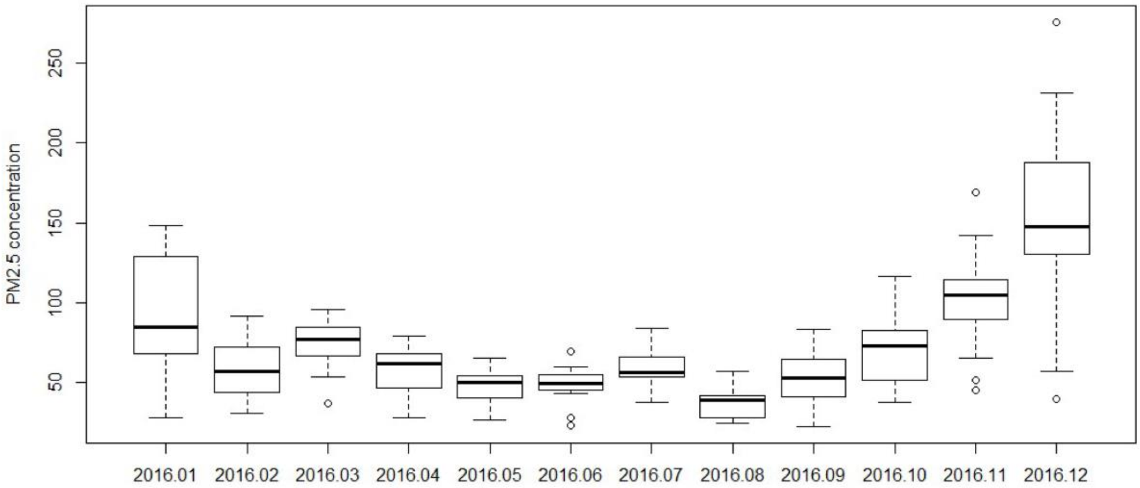


Fig. 1 The monthly average PM2.5 concentrations of cities in the BTH region

3.2 The seasonal variation in characteristics of PM2.5 concentrations

Hourly data of PM2.5 concentrations were collected during spring (from March to May), summer (from June to August), autumn (from September to November) and winter (from December to February), and the quarterly averages and annual averages of PM2.5 concentrations in each city were obtained (see Table 1). The average annual PM2.5 concentration in the BTH region was 69.38 μg·m$^{-3}$, which is far above the secondary standard limit (35 μg.m$^{-3}$) of the Ambient Air Quality Standard. In the same period, the average annual PM2.5 concentration in 338 cities was 47 μg.m$^{-3}$. Furthermore, in the Yangtze River Delta and Pearl River Delta, the average annual PM2.5 concentrations were 46 μg.m$^{-3}$ and 32 μg.m$^{-3}$, respectively, indicating that the PM2.5 pollution in the BTH region is still the most serious among all the studied areas. From the perspective of seasonal changes, the seasonal differences in ambient air pollution in the BTH region were obvious. Specifically, the PM2.5 concentration in winter was approximately twice that in summer, and heavy pollution weather appeared primarily in winter, especially during the heating period. Among the winter months, the PM2.5 concentration in the BTH region was 135 μg.m$^{-3}$ during the heating period from November 15th to December 31st, 2016, which was 2.4 times that of the values during the non-heating period. Five large-scale air pollution processes occurred only in December. From the perspective of the city, PM2.5 concentrations in all cities in the BTH region, except Zhangjiakou, were above the national secondary standards. The annual average PM2.5 concentration in Baoding was the highest at 93.91 μg.m$^{-3}$, which exceeds the national secondary standard limit by 168%.

Seasonal and annual means of the PM2.5 concentration in cities of the BTH region during 2016

| City | *P* (PM2.5)/(μg.m$^{-3}$) | | | | |
|---|---|---|---|---|---|
| | Spring | Summer | Autumn | Winter | Annual mean |
| Beijing | 71.35 | 58.16 | 79.55 | 87.72 | 74.2 |
| Tianjin | 64.95 | 49.01 | 73.68 | 83.16 | 67.7 |
| Shijiazhuang | 65.88 | 45.27 | 122.82 | 121.56 | 88.88 |
| Qinhuangdao | 45.89 | 36.63 | 46.99 | 50.02 | 44.88 |
| Xingtai | 68.31 | 52.99 | 91.25 | 134.67 | 86.81 |
| Handan | 65.17 | 48.24 | 71.69 | 118.13 | 75.81 |
| Baoding | 70.13 | 54.42 | 102.58 | 148.5 | 93.91 |
| Chengde | 40.32 | 30.07 | 40.11 | 52.86 | 40.84 |
| Langfang | 53.08 | 49.45 | 61.87 | 101.68 | 66.52 |
| Zhangjiakou | 30.02 | 28.88 | 34.82 | 30.81 | 31.13 |
| Hengshui | 74.4 | 66.09 | 78.93 | 143.67 | 90.77 |
| Cangzhou | 56.41 | 48.06 | 73.15 | 92.83 | 67.61 |
| Tangshan | 65.4 | 53.03 | 81.78 | 91.13 | 72.84 |
| BTH | 59.33 | 47.72 | 73.79 | 96.67 | 69.38 |

### 3.3 The spatial distribution characteristics of PM2.5 concentration

By using ArcGIS software and the Kriging interpolation method, we evaluated the spatial interpolation of PM2.5 concentrations in the BTH region by month in 2016. The results are shown in Figure 2. The spatial interpolation of the PM2.5 concentration was characterized by severe haze in the southern region, relatively light haze in the northern region and a slightly prominent pattern in some areas. Furthermore, the difference between north and south was large. Southern cities, including Baoding, Shijiazhuang, Xingtai and Handan, within Hebei Province exhibited the highest concentrations. Through the combination of temporal and spatial analysis, we demonstrate that the PM2.5 concentration in the BTH region began to increase from December to February in the following year; haze first appeared in the southern region but expanded to cover the whole area by February. From March to May, the scope of fog and haze narrowed from northwest to the southeast and then remained stable until September. The haze pollution suddenly increased in October and demonstrated a growing trend.

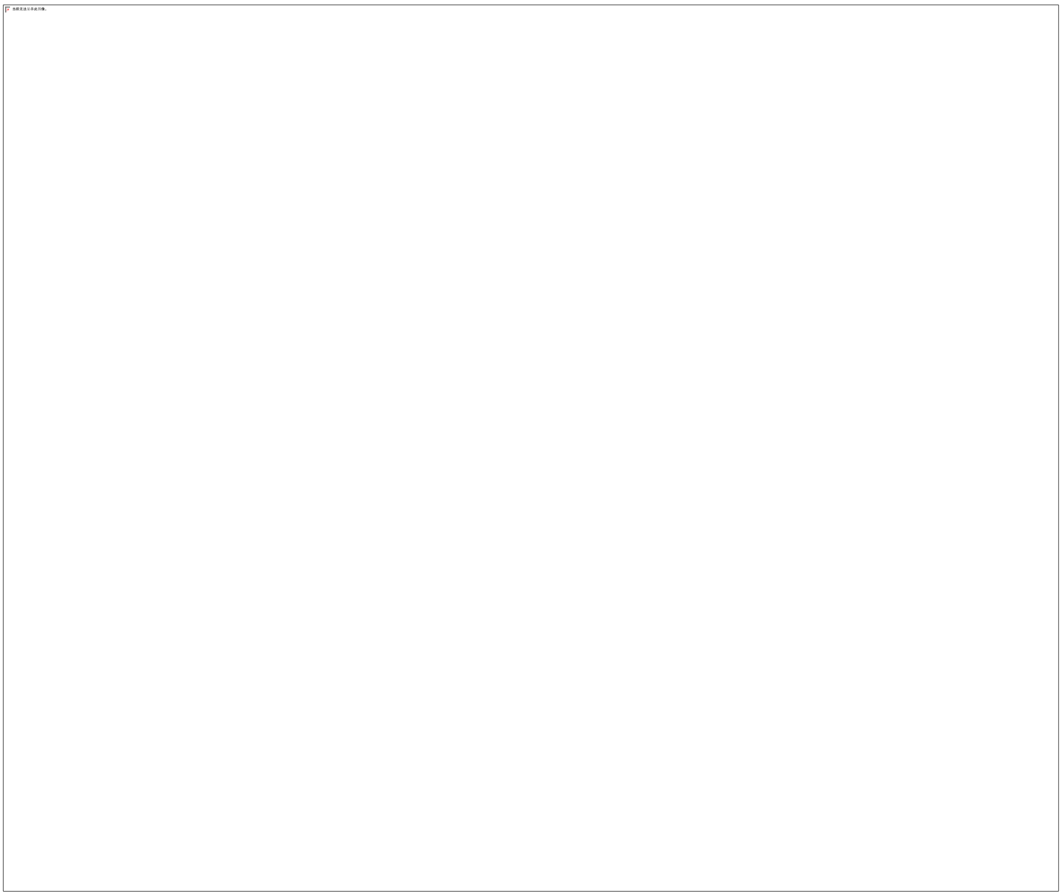

Fig. 2 Spatial distribution of PM2.5 concentrations of cities in the BTH region in 2016

## 4. Results and discussion

### 4.1 Spatial autocorrelation test of the PM2.5 concentration

The global spatial autocorrelation analysis can be used to compare the spatial spillover effect of PM2.5 concentrations within different months. As shown in Table 2, the global Moran Index in terms of the PM2.5 concentration in the BTH region during each of the twelve months from January to December was 2.971, 3.036, 0.732, 1.325, 0.797, 0.181, 2.186, 0.746, 1.190, 1.380, 1.380, 2.482, and 2.372, respectively. These data were obtained using GeoDa software. The Z(I) values of the PM2.5 concentrations were greater than 1.96 in January, February, July, November and December, and the significance test indicated that the PM2.5 concentrations in these months were spatially homogeneous. As a function of season, winter (from December to February of the following year) and summer (from June to August) respectively represent the highest and lowest spatial autocorrelation seasons of the PM2.5 concentration within one year. In other words, the spatial spillover effect is higher in these two seasons than in the other seasons, and PM2.5 pollution is more homogenous during these two seasons

Table 2 Spatial autocorrelation index of PM2.5 concentrations in the BTH region of China in 2016

| Month | Global Moran's Index | Std-err | P-value | Z-stat |
|---|---|---|---|---|
| 1 | 0.493 | 0.193 | 0.001 | 2.971 |
| 2 | 0.495 | 0.194 | 0.001 | 3.036 |
| 3 | 0.039 | 0.176 | 0.213 | 0.732 |
| 4 | 0.144 | 0.179 | 0.103 | 1.325 |
| 5 | 0.056 | 0.181 | 0.208 | 0.797 |
| 6 | 0.117 | 0.184 | 0.305 | 0.181 |
| 7 | 0.321 | 0.183 | 0.014 | 2.186 |
| 8 | 0.049 | 0.182 | 0.218 | 0.746 |
| 9 | 0.126 | 0.186 | 0.126 | 1.190 |
| 10 | 0.155 | 0.177 | 0.084 | 1.380 |
| 11 | 0.322 | 0.167 | 0.013 | 2.482 |
| 12 | 0.354 | 0.186 | 0.012 | 2.372 |

4.2 The spatial pattern evolution characteristics of PM2.5 concentrations in the BTH region

Local spatial autocorrelation analysis was used to analyze the spatial pattern evolution characteristics of PM2.5 pollution and included Moran's Index scatter plot and local indicators of spatial association (LISA) agglomeration analysis. Figure 3 shows the global Moran Index scatter plot for each season of the BTH region in 2016. The abscissa represents standardized PM2.5 concentration in cities, and the ordinate is the neighboring PM2.5 concentration value as determined by the spatial weight matrix based on the Euclidean distance, also known as the space lag vector. The four quadrants of the Moran Index scatter plot represent different agglomeration types. The first quadrant indicates the high-high (HH) agglomeration zone, which means that the PM2.5 concentrations in a city and in its surrounding cities are high. The second quadrant indicates the low-high (LH) aggregation zone, which means that the PM2.5 concentration in a city is low, but values in the surrounding cities are high. The third and fourth quadrants indicate low-low (LL) and high-low (HL) aggregation zones, respectively. The HH and LL agglomeration zones reflect the homogeneity of PM2.5 pollution, which indicates positive spatial autocorrelation. The HL and LH aggregation zones reflect the heterogeneity of PM2.5 pollution, which indicates negative spatial autocorrelation. The spatial correlation of PM2.5 concentration in the BTH region varies with seasons, and the spatial spillover effect in winter is the most significant. The cities with the highest PM2.5 concentration are clustered near the origin point in spring and show strong spatial heterogeneity.

Fig. 3 Global Moran Index scatter plot of PM2.5 concentrations in different seasons

Figure 4 shows that overall, Shijiazhuang, Hengshui and other cities that are located far from the Bohai Bay are HH agglomeration centers. This finding may be due to favorable conditions for air diffusion in coastal cities and to the fact that atmospheric pollutants are easily spread. Meanwhile, Chengde, Qinhuangdao and other coastal cities showed LL agglomeration characteristics, which may be attributed to the low and flat terrain of the southern BTH region, which is not conducive to PM2.5 diffusion. Furthermore, the spatial dependence of the PM2.5 concentration in the urban agglomeration of the BTH region shows a periodic change. During the period from November to February of the following year, the Z-value index was the highest, which indicated that the agglomeration was obvious. This phenomenon is mainly caused by the initiation of coal-fired heating in the northern parts, leading to the spread of PM2.5 from Shijiazhuang and Hengshui to neighboring cities and triggering an increasing area of fog and haze. From March to June, the Z-value index was reduced to the lowest level in the whole year. Because no feature points dominated and the spatial homogeneity was weakened, the range of PM2.5 pollution tended to disappear. From July to October, the scope of the HH agglomeration zone expanded again, and the fine air quality of the northern city tended to be stable. This stability may be caused by the increase in rainfall in summer, which would enhance the purification effect on PM2.5.

Interestingly, a regional haze pollution community has been formed, as the PM2.5 concentration in the BTH region has shown obvious convergence characteristics. This phenomenon may exist because the BTH region is the most concentrated area of China's steel industry, and this industry consumes a great deal of fossil fuel and produces a large amount of industrial emissions. During the autumn and winter of the heating period in the BTH region, coal smoke pollutants caused by industrial boilers and heating boilers increased significantly. Although the atmosphere is stable, the frequency and intensity of inversion is high and thus prone to the agglomeration of pollutants. However, the weather is dry, windy and rainy in the spring, and when summer arrives, the atmospheric stability decreases with concentrated rainfall. Under these conditions, these seasons are not conducive to the formation of concentrated pollutants. Air is a public good without property rights, and despite the serious pollution of fog and haze, regional governments have introduced a large number of high energy-consuming industries in order to develop the economy. Thus, the internal costs have been externalized. There is a linkage between the haze pollution in the cities of the BTH region. If governance measures are implemented only for a single city, the elevated PM2.5 concentration in the surrounding area will still cause the local haze concentration to increase. Therefore, regional joint governance is needed.

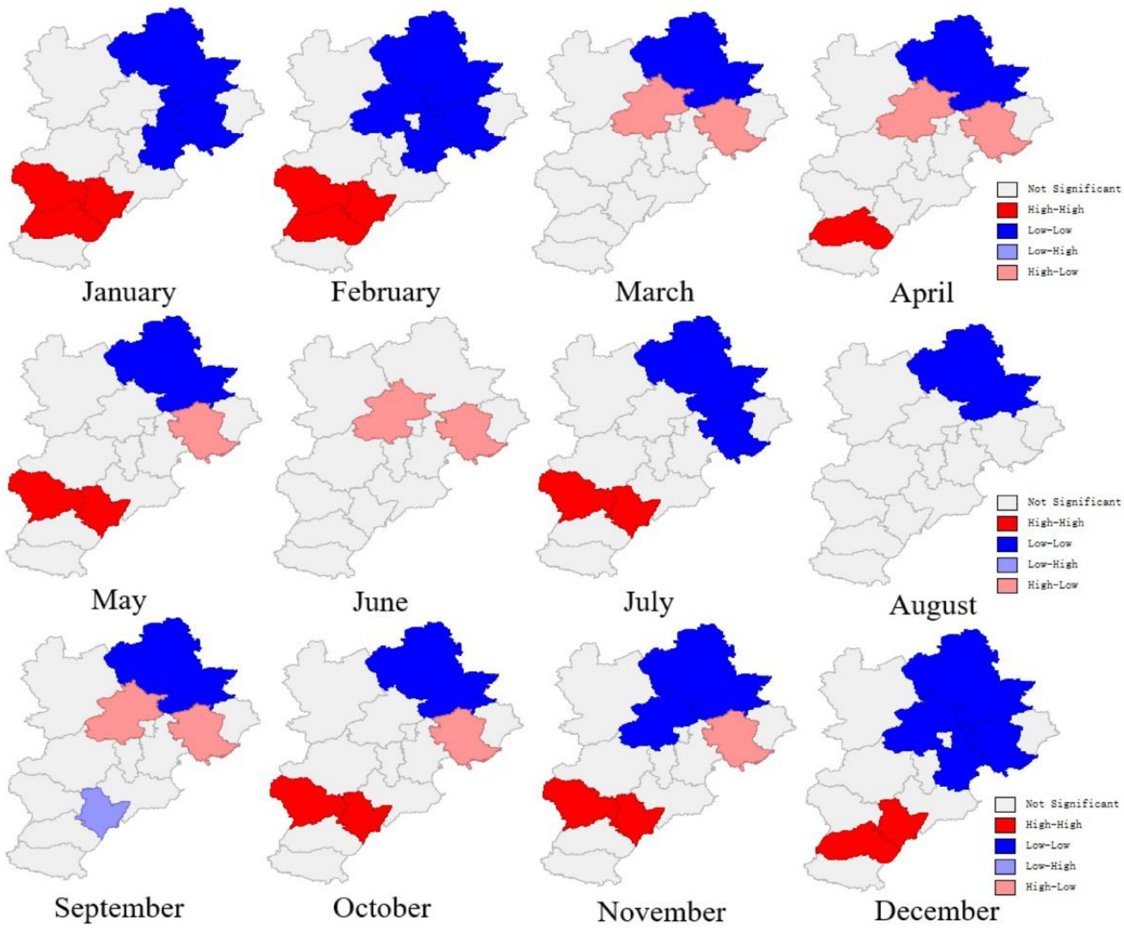


Fig. 4 Monthly spatial agglomeration diagram of PM2.5 concentrations in the BTH region in 2016

## 5. Conclusions and policy implications

The urban agglomeration in the BTH region is a typical haze-prone area, and studying the spatial pattern evolution characteristics of PM2.5 concentrations in the BTH region is important for understanding the mechanism of PM2.5 pollution and the prevention of haze phenomenon. Based on the PM2.5 data released by the China Environmental Monitoring Station, this research analyzed the spatial autocorrelation degree and spatial clustering pattern of PM2.5 concentrations in different seasons of the BTH region based on spatial dependence theory. The primary conclusions are follows.

(1) The distribution of PM2.5 concentrations in this area varied greatly in 2016. On one hand, it increased from late autumn to early winter, and the spatial range

expanded from southeast to northwest. On the other hand, the PM2.5 concentration decreased rapidly from late winter to early spring, and the spatial range was narrowed from northwest to southeast.

(2) The degree of spatial dependence by season was in the following order from highest to lowest: winter, autumn, spring, summer. Winter (from December to February in the following year) and summer (from June to August) were, respectively, the highest and lowest seasons with regard to the spatial homogeneity of PM2.5 concentrations.

(3) The agglomeration pattern of PM2.5 concentrations in the BTH region is significant. Generally, cities such as Shijiazhuang and Hengshui, which are located far from Bohai Bay, exhibited a high-high concentration of PM2.5 pollution, whereas coastal cities, such as Chengde and Qinhuangdao, demonstrated a low-low concentration.

In 2013, the State Council issued the Air Pollution Prevention and Control Action Plan. By 2017, the concentration of fine particles in the BTH region, the Yangtze River Delta and the Pearl River Delta decreased by 25%, 20% and 15% respectively. Among these areas, the BTH region had the most stringent reduction targets because of its severe air pollution. The PM2.5 concentration is the result of the atmospheric reaction of air pollutants, which is affected by atmospheric diffusion conditions. Reducing coal consumption, adjusting energy structure and implementing other initiatives can reduce pollutant emissions, but it is difficult to determine the specific air quality objectives that can be achieved. There are uncertainties in the policy effects of air pollution control programs. Based on the above empirical results, the following suggestions are put forward for haze control in the BTH urban agglomeration. Haze pollution exhibits a linkage relationship in the BTH region. If only a single city is controlled, the high PM2.5 concentration in the surrounding cities will increase the PM2.5 concentration in this city. Therefore, a regional joint governance approach should be adopted. For example, an air pollution joint defense mechanism could be set up for early warning of PM2.5 pollution and rational distribution of pollution control costs among cities in the BTH region through an ecological compensation mechanism. In addition, the haze pollution in the BTH region has two main features. First is the significant spatial difference. The haze pollution in the southern region is relatively more serious, while that in the northern region is relatively light. Second is the significant seasonal difference. The haze during the heating season is serious, while that during the non-heating season is relatively light. Therefore, the policy focus for haze pollution control should be shifted to the control of pollutant discharge in the southern part of the BTH region and should reduce the frequency of severe fog and haze occurrences during the heating season. Finally, monitoring points in the southern region of the BTH region should be increased, and cities far from Bohai Bay, such as Shijiazhuang and Hengshui, should be listed as key cities for prevention and control. Generally, regional joint management is of great value in controlling pollutant emissions and improving the quality of the atmospheric environment. It is necessary to improve the BTH urban agglomeration's collaborative facilities and to promote the integration of the BTH region in order to minimize governance cost.

Presently, existing studies on the PM2.5 concentration in China still concentrate on PM2.5 components, source and space-time phenomena. The factors influencing PM2.5 and its interaction with the urbanization rate based on long-term data are important topics for future research.


## Acknowledgments

The authors express their sincere thanks for the support from the National Natural Science Foundation of China under Grant No. 71173200, the Development and Research Center of China Geological Survey under Grant No. 12120114056601 and No. 12120113093200, the National Science and Technology Major Project under Grant No. 2016ZX05016005-003 and the Fundamental Research Funds for the Central Universities under Grant No. 53200859633.


## Appendix A

Table A1 A Nomenclature List

| Full name | Abbreviation |
| --- | --- |

| | |
|---|---|
| Data Envelopment Analysis | DEA |
| Beijing-Tianjin-Hebei region | BTH region |
| Environmental Kuznets Curve | EKC |
| Air Quality Index | AQI |
| Gross Domestic Product | GDP |
| Inverse Distance Weighted method | IDW method |
| Ordinary Kriging method | OK method |
| High-High agglomeration | HH agglomeration |
| Low-High aggregation | LH agglomeration |
| Low-Low aggregation | LL agglomeration |
| High-Low aggregation | HL agglomeration |
| Local Indicators of Spatial Association | LISA |

Table A2  PM2.5 concentrations in 13 cities in the BTH region by month

| City | 2016.01 | 2016.02 | 2016.03 | 2016.04 | 2016.05 | 2016.06 | 2016.07 | 2016.08 | 2016.09 | 2016.10 | 2016.11 | 2016.12 |
|---|---|---|---|---|---|---|---|---|---|---|---|---|
| Beijing | 68.15 | 43.48 | 92.67 | 67.54 | 53.85 | 59.28 | 68.6 | 46.6 | 54.63 | 84.73 | 99.3 | 130.55 |
| Tianjin | 73.52 | 50.29 | 80.84 | 63.35 | 50.65 | 53.32 | 52.97 | 40.75 | 52.47 | 64.07 | 104.49 | 134.9 |
| Shijiazhuang | 129.63 | 71.61 | 83.16 | 60.33 | 54.15 | 44.91 | 65.72 | 25.18 | 83.02 | 116.4 | 169.03 | 276.06 |
| Qinhuangdao | 40.2 | 38.09 | 63.57 | 39.36 | 34.73 | 42.53 | 39.75 | 27.62 | 36.49 | 39.65 | 64.83 | 84.3 |
| Xingtai | 129.09 | 81.34 | 88.2 | 66.1 | 50.64 | 54.17 | 65.86 | 38.95 | 67.35 | 82.23 | 124.17 | 188.04 |
| Handan | 108.58 | 72.3 | 75.09 | 78.67 | 41.76 | 48.75 | 54.73 | 41.23 | 56.12 | 50.87 | 108.07 | 231.65 |
| Baoding | 148.28 | 83.37 | 76.78 | 68.23 | 65.37 | 54.46 | 70.95 | 37.85 | 69.35 | 96.25 | 142.13 | 189.99 |
| Chengde | 44.79 | 40.86 | 53.25 | 37.63 | 30.07 | 27.56 | 37.13 | 25.52 | 27.59 | 41.66 | 51.07 | 56.73 |
| Langfang | 88.45 | 50.74 | 73.08 | 46.09 | 40.07 | 48.9 | 56.38 | 43.08 | 41.07 | 55.29 | 89.25 | 151.21 |
| Zhangjiakou | 27.52 | 30.14 | 36.49 | 27.45 | 26.11 | 22.87 | 39.78 | 24 | 22.08 | 37.59 | 44.8 | 39.25 |
| Hengshui | 133.78 | 91.38 | 95.28 | 72.41 | 55.52 | 58.11 | 83.57 | 56.59 | 47.27 | 75.19 | 114.34 | 159.27 |
| Cangzhou | 84.17 | 56.59 | 66.63 | 57.25 | 45.36 | 46.79 | 56.25 | 41.13 | 43.93 | 72.87 | 102.64 | 142.25 |

| | | | | | | | | | | | | |
|---|---|---|---|---|---|---|---|---|---|---|---|---|
| Tangshan | 78.32 | 58.92 | 84.6 | 61.53 | 50.07 | 69.52 | 55.2 | 34.38 | 64.04 | 72.96 | 108.33 | 147.34 |

## References


Alves C, Vicente A, Pio C, et al. Organic compounds in aerosols from selected European sites–Biogenic versus, anthropogenic sources[J]. Atmospheric Environment, 2012, 59(59):243-255.

Bates D V, Sizto R. Air pollution and hospital admissions in Southern Ontario: the acid summer haze effect[J]. Environmental research, 1987, 43(2): 317-331.

Cai S, Wang Y, Zhao B, et al. The impact of the "Air Pollution Prevention and Control Action Plan" on PM2.5 concentrations in Jing-Jin-Ji region during 2012-2020[J]. Science of the Total Environment, 2017, 580:197-209.

Chalbot M C G, Jones T A, Kavouras I G. Trends of non-accidental, cardiovascular, stroke and lung cancer mortality in Arkansas are associated with ambient PM2.5 reductions[J].

Civan M Y, Elbir T, Seyfioglu R, et al. Spatial and temporal variations in atmospheric VOCs, NO2, SO2, and O3 concentrations at a heavily industrialized region in Western Turkey, and assessment of the carcinogenic risk levels of benzene[J]. Atmospheric Environment, 2015, 103: 102-113.

Dockery D W, Pope C A, Xu X, et al. An association between air pollution and mortality in six US cities[J]. New England journal of medicine, 1993, 329(24): 1753-1759.

Guan D, Su X, Zhang Q, et al. The socioeconomic drivers of China’s primary PM2.5 emissions[J]. Environmental Research Letters, 2014, 9(2): 024010.

Hao Y, Liu Y M. The influential factors of urban PM 2.5 concentrations in China: a spatial econometric analysis[J]. Journal of Cleaner Production, 2016, 112: 1443-1453.

Hsu C Y, Chiang H C, Chen M J, et al. Ambient PM2.5 in the residential area near industrial complexes: Spatiotemporal variation, source apportionment, and health impact.[J]. Science of the Total Environment, 2017.

Hu W, Downward G S, Reiss B, et al. Personal and indoor PM2.5 exposure from burning solid fuels in vented and unvented stoves in a rural region of China with a high incidence of lung cancer[J]. Environmental science & technology, 2014, 48(15): 8456-8464.

Hussain S Q, Ahn S H, Park H, et al. Light trapping scheme of ICP-RIE glass texturing by SF 6/Ar plasma for high haze ratio[J]. Vacuum, 2013, 94: 87-91.

Jansen R C, Shi Y, Chen J, et al. Using hourly measurements to explore the role of secondary inorganic aerosol in PM2.5 during haze and fog in Hangzhou, China[J]. Advances in Atmospheric Sciences, 2014, 31(6): 1427-1434.

Lee S J, Serre M L, van Donkelaar A, et al. Comparison of geostatistical interpolation and remote sensing techniques for estimating long-term exposure to ambient PM2.5 concentrations across the continental United States.[J]. Environmental health perspectives, 2012, 120(12): 1727.

Li L, Yang J, Song Y F, et al. The burden of COPD mortality due to ambient air pollution in Guangzhou, China[J]. Scientific reports, 2016, 6.

Liao T, Wang S, Ai J, et al. Heavy pollution episodes, transport pathways and potential sources of PM2.5 during the winter of 2013 in Chengdu (China).[J]. Science of the Total Environment, 2017, 584-585:1056.

Liu C, Henderson B H, Wang D, et al. A land use regression application into assessing spatial variation of intra-urban fine particulate matter (PM 2.5) and nitrogen dioxide (NO2 ) concentrations in City of Shanghai, China[J]. Science of the Total Environment, 2016, 565:607-615.

Liu Q, Wang Q. Sources and flows of China's virtual SO2, emission transfers embodied in interprovincial trade: A multiregional input–output analysis[J]. Journal of Cleaner Production, 2017, 161.

Liu Z, Cheng K, Li H, et al. Exploring the potential relationship between indoor air quality and the concentration of airborne culturable fungi: a combined experimental and neural network modeling study[J]. Environ Sci Pollut Res Int, 2017b(6):1-8.

Liu Z, Hu B, Wang L, et al. Seasonal and diurnal variation in particulate matter (PM 10, and PM 2.5 ) at an urban site of Beijing: analyses from a 9-year study[J]. Environmental Science and Pollution Research, 2015a, 22(1):627-642.

Liu Z, Li H, Cao G. Quick estimation model for the concentration of indoor airborne culturable bacteria: an application of machine learning[J]. International Journal of Environmental Research and Public Health, 2017a, 14(8): 857.

Liu Z, Zhu Z, Zhu Y, et al. Investigation of dust loading and culturable microorganisms of HVAC systems in 24 office buildings in Beijing[J]. Energy and Buildings, 2015b, 103: 166-174.

Luo J, Du P, Samat A, et al. Spatiotemporal Pattern of PM2.5 Concentrations in Mainland China and Analysis of Its Influencing Factors using Geographically Weighted Regression[J]. Scientific Reports, 2017, 7.

Ma M, Shen L, Ren H, et al. How to Measure Carbon Emission Reduction in China’s Public Building Sector: Retrospective Decomposition Analysis Based on STIRPAT Model in 2000–2015[J]. Sustainability, 2017c, 9(10): 1744.

Ma M, Yan R, Cai W. An extended STIRPAT model-based methodology for evaluating the driving forces affecting carbon emissions in existing public building sector: evidence from China in 2000–2015[J]. Natural Hazards, 2017b, 89(2): 741-756.

Ma M, Yan R, Du Y, et al. A methodology to assess China's building energy savings at the national level: An IPAT–LMDI model approach[J]. Journal of cleaner production, 2017a, 143: 784-793.

Moroń W, Rybak W. NOx and SO2 emissions of coals, biomass and their blends under different oxy-fuel atmospheres[J]. Atmospheric Environment, 2015, 116: 65-71.

National Bureau of Statistics of the People's Republic of China. Hebei Economic Yearbook 2014[M]; China Statistical Press:Beijing, China, 2014.

National Bureau of Statistics of the People's Republic of China. Beijing statistical yearbook 2014[M]; China Statistical Press:Beijing, China, 2014.

National Bureau of Statistics of the People's Republic of China. Tianjin statistical yearbook 2014[M]; China Statistical Press:Beijing, China, 2014.

Shuai C, Shen L, Jiao L, et al. Identifying key impact factors on carbon emission: evidences from panel and time-series data of 125 countries from 1990 to 2011[J]. Applied Energy, 2017, 187: 310-325.

Su B, Thomson E. China's carbon emissions embodied in (normal and processing) exports and their driving forces, 2006–2012[J]. Energy Economics, 2016, 59: 414-422.

Tobler W R. A computer movie simulating urban growth in the Detroit region[J]. Economic geography, 1970, 46(sup1): 234-240.

Wang X, Ding X, Fu X, et al. Aerosol scattering coefficients and major chemical compositions of fine particles observed at a rural site in the central Pearl River Delta, South China[J]. Journal of Environmental Sciences, 2012, 24(1): 72-77.

Wang Y S, Yao L, Wang L L, et al. Mechanism for the formation of the January 2013 heavy haze pollution episode over central and eastern China[J]. Science China Earth Sciences, 2014, 57(1): 14-25.

Wang Z, Fang C, Guang X U, et al. Spatial-temporal characteristics of the PM_(2.5) in China in 2014[J]. Acta Geographica Sinica, 2015 (in Chinese).

Wu J, Li J, Peng J, et al. Applying land use regression model to estimate spatial variation of PM2.5 in Beijing, China[J]. Environmental Science and Pollution Research, 2015, 22(9): 7045-7061.

Wu X, Chen Y, Guo J, et al. Spatial concentration, impact factors and prevention-control measures of PM2.5 pollution in China[J]. Natural Hazards, 1-18.

Xu B, Lin B. Regional differences of pollution emissions in China: contributing factors and mitigation strategies[J]. Journal of Cleaner Production, 2015, 112(4):1454-1463.

Yan D, Lei Y, Li L, et al. Carbon emission efficiency and spatial clustering analyses in China’s thermal power industry: Evidence from the provincial level[J]. Journal of Cleaner Production, 2017.

Yan R, Ma M, Pan T. Estimating energy savings in Chinese residential buildings from 2001 to 2015: A decomposition analysis[J]. Journal of Engineering Science & Technology Review, 2017, 10(1).

Zhang A, Qi Q, Jiang L, et al. Population exposure to PM 2.5 in the urban area of Beijing[J]. PloS one, 2013, 8(5): e63486.

Zhang Y J, Hao J F, Song J. The CO2 emission efficiency, reduction potential and spatial clustering in China’s industry: evidence from the regional level[J]. Applied Energy, 2016, 174: 213-223.

Zhao B, Wang P, Ma J Z, et al. A high-resolution emission inventory of primary pollutants for the Huabei region, China[J]. Atmospheric Chemistry & Physics, 2012, 11(1):20331-20374.

Zhao X, Wang X, Ding X, et al. Compositions and sources of organic acids in fine particles (PM2.5) over the Pearl River Delta region, south China[J]. Journal of Environmental Sciences, 2014, 26(1): 110-121.

Zhao Y, Liu Y, Ma J, et al. Heterogeneous reaction of SO2 with soot: The roles of relative humidity and surface composition of soot in surface sulfate formation[J]. Atmospheric Environment, 2017, 152: 465-476.

Zou B, Wang M, Wan N, et al. Spatial modeling of PM 2.5, concentrations with a multifactoral radial basis function neural network[J]. Environmental Science and Pollution Research, 2015, 22(14):10395-404.